Assessment of the Mechanical Properties of the Musculoskeletal System Using 3-D Very High Frame Rate Ultrasound

Thomas Deffieux, Jean-Luc Gennisson, Mickaël Tanter, and Mathias Fink

Abstract—**One of the great challenges for understanding muscular diseases is to assess noninvasively the active and passive mechanical properties of the musculoskeletal system. In this paper we report the use of ultrafast ultrasound imaging to explore with a submillimeter resolution the behavior of the contracting tissues *in vivo* (biceps brachii). To image the contraction, which is a very brief phenomenon (<100 ms), a recently designed ultrasound scanner prototype able to take up to 6000 frames/s was used. A very high frame rate from 1000 to 2500 frames/s was used to image the cross section plane of the muscle (transverse to fibers) enabling us to catch in real time the muscle contraction during a transient electrostimulation. Tissue velocities were obtained from radio frequency-based speckle tracking techniques and their profiles are discussed with respect to electrostimulation intensities and pulse repetition frequencies for different volunteers. Three-dimensional (3-D) very high frame rate movies were also acquired by repeating the experiment for different acquisition planes while triggering the imaging system with the electrostimulation device. The reconstructed 3-D velocity field allows the full localization of the contracting fibers bundle. This ultrasound technique, referred to as echo mechanomyography, offers new perspectives for *in vivo* and *in situ* noninvasive muscle diagnosis of an active contractile tissue.**

I. Introduction

Measurement methods of muscle properties are of great clinical interest for physical therapists seeking to diagnose muscle diseases and plan accurate treatments. They are also very helpful to narrow the search for genetic disorders by improving the diagnosis [1].

Among these methods, some are specifically designed and are fully dedicated to the measurement of muscle functional properties, such as electromyography (EMG), which records the muscle electrical activity [2], and surface mechanomyography [3] (sMMG) or acceleromyography [4], which records pressure or acceleration on the skin surface during a contraction. Electromyography is a powerful tool to discriminate between neuromuscular and physiological disorders by recording the compound action potential with a needle electrode or by using surface electrodes. Presence at rest as well as size and shape of the action potentials are all key factors in the diagnosis of a neuromuscular disease [2], especially neuropathies and myopathies.

Standard imaging techniques have also been applied and adapted to the muscle. They provide full anatomic as well as functional images of the muscle. Among them are mainly T1 and T2 weighted magnetic resonance (MR) imaging [5], MR spectroscopy [6], cine phase contrast MR imaging [7], MR elastography [8], Doppler imaging [9], and ultrasonography [10]. Although they provide valuable information on different functional parameters of the muscle, many of them, too expensive, are not yet used clinically and are still in an early research phase. **[AU1: AuQ; No Ref. 11 here or in References. Refs have been renumbered, please proof carefully.]**

Based on the tissue velocity field estimation during contraction, cine phase contrast MR [7] or ultrasound Doppler [9] present new functional imaging techniques of the mechanical activity of a muscle and are thus complementary to electromyography which measures its electrical activity and a natural extension to mechanomyography which records the mechanical activity at the surface. Unfortunately, those techniques lack a good time resolution and can only image slow mechanical response of the muscle; therefore they are blind to transient phenomena occurring during a muscle contraction such as those recorded by EMG [11] or sMMG [12].

High frame rate ultrasound techniques (>100 Hz) are able to track small displacements noninvasively with both good spatial and good temporal resolutions. In 2004, Witte *et al.* conducted an experiment with a single ultrasound element on an electrostimulated *ex vivo* rat muscle, demonstrating the use of radio frequency (RF)-based speckle tracking techniques to record an *in situ* contraction with a high sampling rate [13]. In 2006, another experiment was devoted to the role of fatigue with the imaging of an *in vivo* contraction of the flexor digitorum superficialis muscle with an iU22 scanner able to reach 320 images per second [14]. Also in 2006, Deffieux *et al.* published a proof of concept paper demonstrating the feasibility of using ultrafast ultrasound imaging to track the *in vivo* contraction of the biceps brachii [15]. Beyond tetanization or fatigue study, this approach results in both localization of the contracting fiber bundle and extraction of the temporal profile of the tissue velocity field inside the contracting fiber bundle. This technique was named echo mechanomyography (eMMG) in reference to sMMG.

Manuscript received August 13, 2007; accepted February 29, 2008.

The authors are with the Laboratoire Ondes et Acoustique, ESPCI, CNRS UMR 7587, INSERM, Université Paris VII, 75231 Paris Cedex 05, France (e-mail: thomas.deffieux@espci.fr).

Digital Object Identifier 10.1109/TUFFC.

In the present paper, we aim to consolidate these findings and investigate the repeatability of eMMG with a new ultrafast ultrasound scanner. Based on research on transient elastography [16], our new ultrafast ultrasound scanner prototype can store up to 1000 ultrafast echographic frames with a framerate ranging from 500 up to 20,000 frames/s. The acquisition is synchronized with an electrostimulation device. The contraction can thus be fully imaged and its associated tissue velocity field recorded in a region of interest (ROI) of the image. The maxima of the tissue velocity field perpendicular to the fiber muscle are found to be a quadratic function of the stimulation amplitude.

An experimental setup is also proposed enabling a three-dimensional (3-D) acquisition of the velocity field, providing a much better spatial localization of the contracting fiber bundle. The feasibility of this imaging technique is demonstrated *in vivo* and discussed, as well as the results and the difficulties of these preliminary sets of experiments. Finally, in vivo assessment of the propagation speed of mechanical tissue displacements induced by transient electrostimulations was measured in healthy volunteers ($v \approx 4$ m.s^{-1}) and compared with the propagation speed of shear waves induced in the same area using a remote ultrasonic radiation force (v ranging from 2.5 m.s^{-1} at rest to 5 m.s^{-1} for a 4 kg loading).

By adding information on the mechanical response of the muscle, we hope that the technique can turn into a powerful tool complimentary to electromyography and can extend surface mechanomyography, resulting in a measuring technique taking into account the whole command–response chain of the muscle system *in situ*.

II. Materials and Methods

A. Muscle

Experiments were focused on the biceps brachii, a muscle of the arm controlling elbow flexion as well as wrist supination. The biceps lies just under the skin and is innervated by the musculocutaneous nerve. Its motor point, the nerve entry into the muscle, is usually located midway of the muscle, between the shoulder and the elbow (Fig. 1).

Muscle contraction is a complex electromechanical phenomenon, which is controlled by the nervous system. An action potential propagating along a motoneuron of the nerve is chemically transmitted to a muscle fiber at the neuromuscular junction. Each motoneuron can control several muscle fibers constituting a single motor unit. The transmitted action potential then propagates along the muscle fiber membrane, the sarcolemma, and initiates an entry of calcium ions into the muscle fiber cytoplasm [17]. The calcium then binds to the troponin–tropomyosin molecules allowing myosin molecules to freely interact with actin, an interaction that develops force (Fig. 2). Calcium is then pumped out of the cell, and adenosine triphosphate (ATP) is used to reset the actin–myosin complex to its initial state [18]. Contraction propagates along a muscle fiber with the action potential at a few meters per second, as measured by the muscle fiber conduction velocity (MFVC) technique [11], a special mode of electromyography.

The whole contraction process lasts less than one hundred milliseconds depending on the fiber type [19]; it is thus very difficult to image as a single mechanical event by traditional imaging techniques, although it can easily be electrically recorded by an electromyography system (single motor unit action potential recording) or surface mechanomyography.

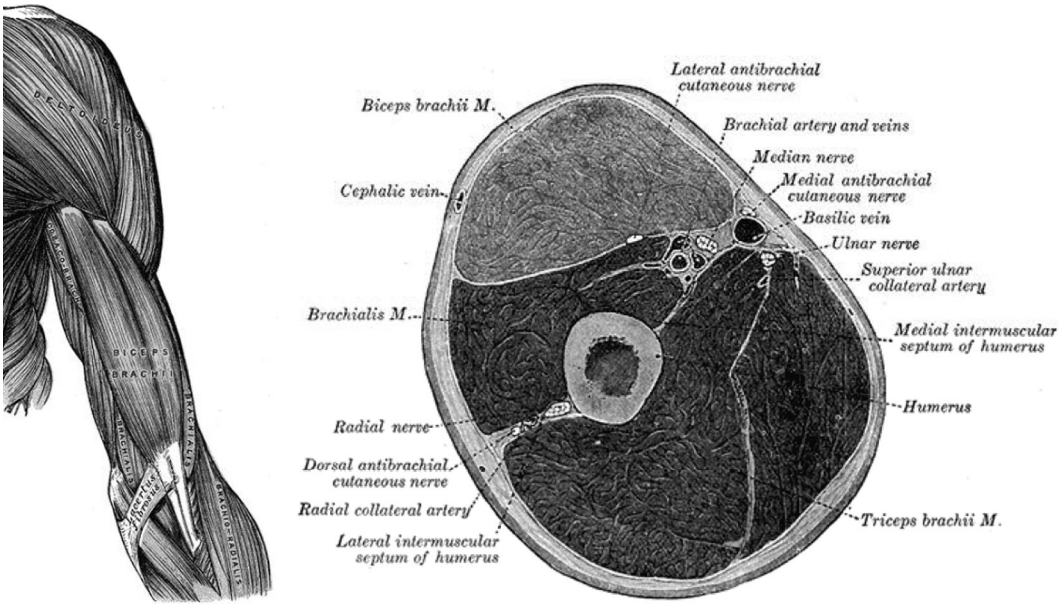

Fig. 1. Anatomy of the arm. The biceps brachii is highlighted in red. The image was taken from the 1918 edition of *Gray's Anatomy*.

B. Imaging Device

The technique is based on the use of an ultrafast scanner coupled with an electrostimulation device. The electrostimulation device is used to allow a perfect synchronization of the contraction with the acquisition. Moreover, the electrostimulation device allows a repeat of the acquisition under the same conditions, enabling a stroboscopic 3-D scan as well as evaluation of the repeatability.

The ultrasonic scanner used for these measurements is a prototype designed by SuperSonic Imagine Company (Aix en Provence, France) for clinical trials of the supersonic shear imaging technique (an imaging technique capable of indicating the shear modulus of *in vivo* tissue and based on the coupling between ultrafast echographic sequences and remote palpation induced by the ultrasonic radiation force [20]). This scanner offers a medical grade image quality, ultrafast imaging as well as a Matlab api (The MathWorks, Inc., Natick, MA) and has been approved for clinical trials. This scanner was coupled with a 5 Mhz linear transducer array (4 to 7 MHz bandwidth; L7–4, ATL, Seattle, WA).

Applying ultrasound imaging to the acquisition of the muscular contraction requires mainly 3 conditions:

- A submillimetric resolution to obtain good image quality and good localization of structures inside the muscle; this is generally achieved by all conventional ultrasound scanners.
- A high frame rate to track the modification of the muscle in a very short period of time during the contraction (lasting less than 100 ms). This translates into frame rates higher than 200 Hz (for 20 samples). Very high frame rates (>500 Hz) improve the sampling time, enabling more accurate measurements of contraction and half relaxation times. This is also required in order to measure the velocity of the propagation of the contraction, which is expected to follow the muscle fiber conduction velocity close to 4 m/s [11]. A propagation distance of about 2 cm results in a time delay of 5 ms from end to end and as such requires at least 2000 Hz for a delay of 10 samples.
- A micrometer sensitivity to displacement between consecutive ultrasound images. For high frame rates, displacements appear smaller requiring higher accuracy in their measurements. It is also possible to correlate nonconsecutive ultrasound images to reach a lower frame rate to increase the apparent amplitude of the displacements; however, this operation is similar to that of a low pass filter [21]. In practice, we use consecutive images keeping the full bandwidth of the acquired signal.

The physical principle behind ultrafast imaging is to reach very high frame rates by using plane wave insonifications of the medium instead of the conventional line per line focusing techniques. Single plane wave insonifications are known to decrease the B-mode image quality but allow much higher frame rates because only one transmit step is needed to build a full image.

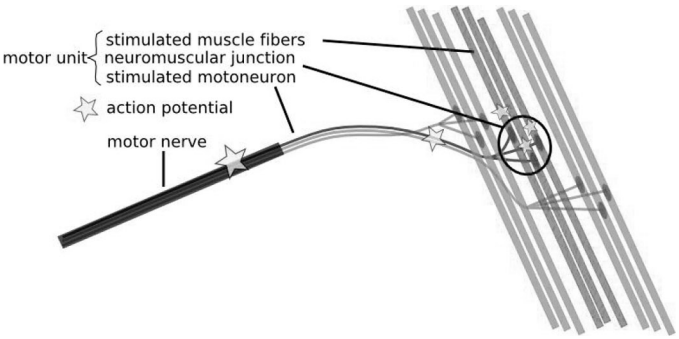

Fig. 2. Illustration of the neuromuscular complex. An action potential propagates along a stimulated motoneuron to the neuromuscular junction. It is then transmitted to the muscle fibers belonging to the same motor unit and triggers the contraction of sarcomeres while propagating.

Backscattered signals are then directly stored in the device's memories, and images are reconstructed in a post-processing step using a conventional beamforming technique, that is to say, applying a time delay operation to compensate for the travel times differences.

The velocity field is then estimated from 2, usually consecutive, frames by applying one-dimensional cross-correlations of windows of the RF signal along the beam axis (RF signals are sampled at a much higher sampling rate and thus feature a much higher precision than the envelope signal), a technique known as RF-based speckle tracking [22]. The scanner performs an automatic In phase (I) and Quadrature (Q) demodulation of the acquired signals at the central frequency:

$$S_i(x,t) = I_i(x,t) \times \cos(\omega_{us} t) + Q_i(x,t) \times \sin(\omega_{us} t), \quad (1)$$

where S_i is the conventional beamformed ultrasound signal (t being along the beam axis and x along the transducers), and I_i and Q_i represent the In phase and Quadrature demodulated and beamformed signals as stored by the scanner for the i^{th} image. At the same time, the RF-based speckle tracking step is directly implemented as a phase shift $d\phi$ estimation along the beam axis between 2 ultrasound images:

$$d\varphi_{i \to i+k}(x,t) = \frac{\mathbf{1}}{\omega_{us}} \tan^{-1}\left(\frac{\mathbf{Q}_i(x,t)\mathbf{I}_{i+k}(x,t) - \mathbf{I}_i(x,t)\mathbf{Q}_{i+k}(x,t)}{\mathbf{I}_i(x,t)\mathbf{I}_{i+k}(x,t) + \mathbf{Q}_i(x,t)\mathbf{Q}_{i+k}(x,t)} \right), \quad (2)$$

where the phase shift $d\phi$ can be computed from the In phase and Quadrature signals for the i^{th} and the $i{+}k^{\text{th}}$ images. When higher accuracy is required and time sampling is not critical, the lag k between the ultrasound images can be increased; the result is then equivalent to a high sampled signal but filtered with a low-pass sliding window. In practice, we used consecutive images ($k = 1$), keeping the original bandwidth of the signal. One can then esti-

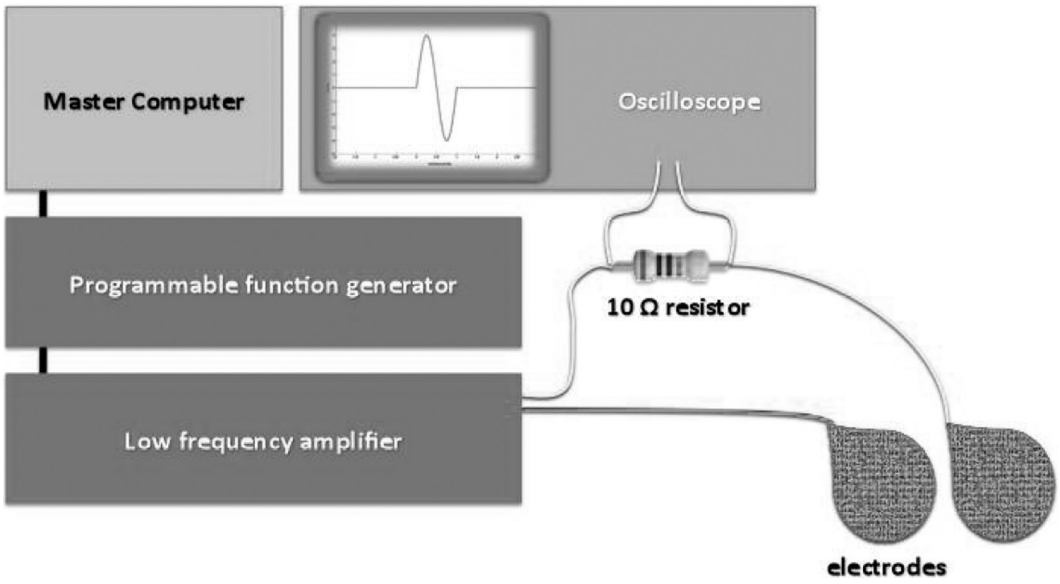

Fig. 3. Schema of the electrostimulation setup. The programmable function generator's output is connected to a low frequency amplifier, which is directly connected to the electrodes. The monitoring of the tension of a 10 Ω resistor in series allows a check of the intensity used. Electrodes are positioned on the biceps brachii, one over the motor point and one near the elbow.

mate the z component of the tissue velocity field V_z from the phase shift $d\phi$ between successive images:

$$Vz(x,z,i) = \frac{1}{2} \times \frac{d\varphi_{i \to i+k}(x,t)}{2\pi} \times \lambda_{\text{us}} \times \frac{F_{\text{im}}}{k}, \qquad (3)$$

where λ_{us} is the ultrasound wavelength, $z = c_{\text{us}}.t$ is the depth, F_{im} is the imaging frame rate, and k is the lag between compared images.

One can notice that the measured tissue velocity field V_z is only the component parallel to the beam axis z of the true tissue velocity vector V and that a displacement superior to half the wavelength ($d\phi > 2\pi$) requires unwrapping. The high frame rate enables us to track smaller movements but also to record higher frequency signals more accurately, thanks to an increased sampling rate.

C. Electrostimulation Device

An electrostimulation device was used to trigger the contraction in order to enhance repeatability, synchronization, and better overall control over a voluntary contraction (Fig. 3). The[**AU2: Most figures were not cited in text. Please carefully review all figure citations and correct as needed.**] electrostimulation was set up to be triggered by the imaging device through a standard TTL entry, thus avoiding any additional delay in the experimental setup. The electrostimulation device was composed of a programmable function generator (Model 33220A; Agilent Technologies, Inc., Palo Alto, CA) controlled by a computer through a GPIB interface, a low frequency amplifier (Type 2718; Brüel & Kjær, Nærum, Denmark), an oscilloscope (Tectronix, Inc., Dyersburg, TN), and a pair of noninvasive surface electrodes. Electrical pulse duration was set to 1 ms. A 10 Ω resistor was put in series with the electrodes and its tension was visualized on the oscilloscope to measure the corresponding intensity.

Electrodes had to be carefully placed to excite the nerve on the motor point of the biceps brachii, a well-innervated region of the muscle where contraction is maximal for a given excitation. Applying an electric stimulation on the motor point leads to the depolarization of some motor axons of the nerve. An action potential is then generated in each excited axon and propagates to the end motor plates of the axon where it is transmitted to associated muscle fibers. Each axon is connected to several adjacent muscle fibers forming a single coherent motor unit. The transmitted action potential propagates on the surface of each excited muscle fiber and makes it twitch, resulting in a short and small contraction of the fiber (Fig. 2). Depending on the number of recruited motor units and their firing rate, different contraction strengths can be generated. That being said, electrostimulation is always heavily dependent on the position of the electrodes and the muscle state regarding its efficiency and localization [23].

To fine-tune the electrostimulation, the voltage was gradually incremented and the local tissue velocity analyzed as a function of time and current values; all of these measurements have been fully automatized through the use of the GPIB interface. Voltages used were typically around a few volts (corresponding to a few mA), a tradeoff between signal-to-noise ratio in the velocity field and the locality (to avoid excitation of many motor units resulting in a large contraction). In these experiments, we tried to have a small excitation corresponding to the activation of a few motor units while keeping a reasonable signal-to-noise ratio.

Since the muscle is also a viscoelastic medium [8], [24], a dilatation of one area compresses the surrounding tissue according to the boundary conditions (bone, skin, tendon, or other soft tissues) resulting in a complex tissue velocity

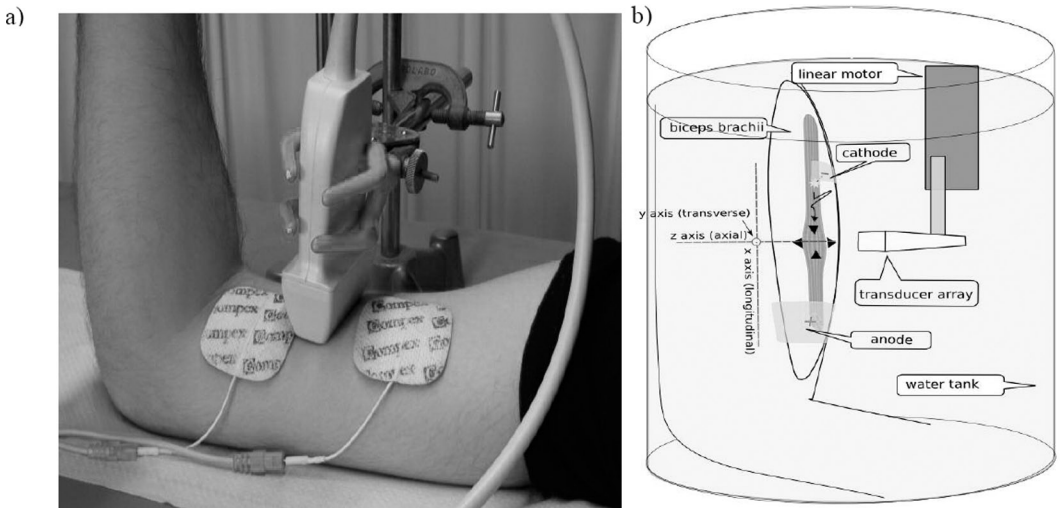

Fig. 4. Experimental setup for a 2D single acquisition (a) or a full 3-D scan (b). The imaging probe is positioned perpendicular to the muscle fibers in both cases and can be translated in the 3-D case. A few-millimeter layer of gel was inserted between the probe and the muscle to avoid contact during contraction.

field. Smaller contractions enable us to avoid most of the hard boundary conditions and remain local. However, all hard boundary effects could not be avoided and a twist of the excited muscle fiber is visible in most experiments and will be discussed later.

D. Experimental Setups

A master computer controls both the imaging device and the electrostimulation device. Running the ultrafast imaging sequence automatically launches the electrostimulation device through a hardware trigger. The probe was always positioned perpendicularly to the bone, meaning the imaging plane was a transverse cross section in regard to the fiber's main axis [Fig. 4(a)].

As noted previously, the measured tissue velocity corresponds only to the component parallel to the ultrasound beam axis of the true tissue velocity vector. This means that the measured tissue velocity was always perpendicular to the bone and thus perpendicular to the muscle fibers. However, a contracting fiber is naturally shortening in its longitudinal direction, thus mainly creating a displacement of the tissue in the longitudinal direction, a displacement that cannot be imaged precisely by our system. Fortunately, while contracting, the fiber also happens to grow in diameter explaining why a muscle increases in diameter when contracting. The empiric law linking the lateral stretch to the longitudinal stretch can be written [25]:

$$\lambda_{\text{lateral}} = \frac{1}{\sqrt{\lambda_{\text{longitudinal}}}}. \tag{4}$$

The first set of experiments was dedicated to a single twitch while slowly increasing the stimulation amplitude. The experiment was then repeated on 3 healthy volunteers and the repeatability discussed. As a true imaging technique, geometrical and spatial extension can be fully visualized. Contraction and relaxation times were also extracted for each volunteer and their physiological meaning discussed. The imaging sequence was set to 1000 frames per second for 300 images.

In a second experiment, the electrostimulation pulse repetition was increased to induce a tetany of the muscle. The velocity profiles were then extracted for each frequency. For this experiment, 1000 images were acquired at 1000 frames per second.

Finally, a 3-D setup was also developed and tested to allow the imaging of the whole contracting bundle and follow any propagation that could occur along the fiber axis (Fig. 4). To perform such a scan of the biceps brachii, we used a linear motor (Micos; SMC Pollux, Freiburg, Germany) moved along the bone axis and took an ultrafast acquisition in the transverse plane at each position [Fig. 4(b)]. Ultrafast acquisitions were performed at 2000 or 2500 frames/s and was set up to trigger the electrostimulation device. The electrical stimulation was thus repeated for each position and a 3-D movie of the contraction was computed.

III. Results

A. Electrostimulation Amplitude and Recruitment

1. Measurement of Tissue Velocity Profile: We tried to keep the excitation as small as possible to have only a small region of the biceps contracting and to keep a local response, thus avoiding boundary conditions and complex movements of the muscle. Transverse images show a good localization of the maximum of the contracting fiber bundle that will lay the grounds for the 3-D tracking of the contracting fiber bundle. The velocity profile was extracted from the mean inside a 3×3 mm^2 square positioned as close as possible to the maximum [Fig. 5(a)]. The measured intensity through the resistor also happens

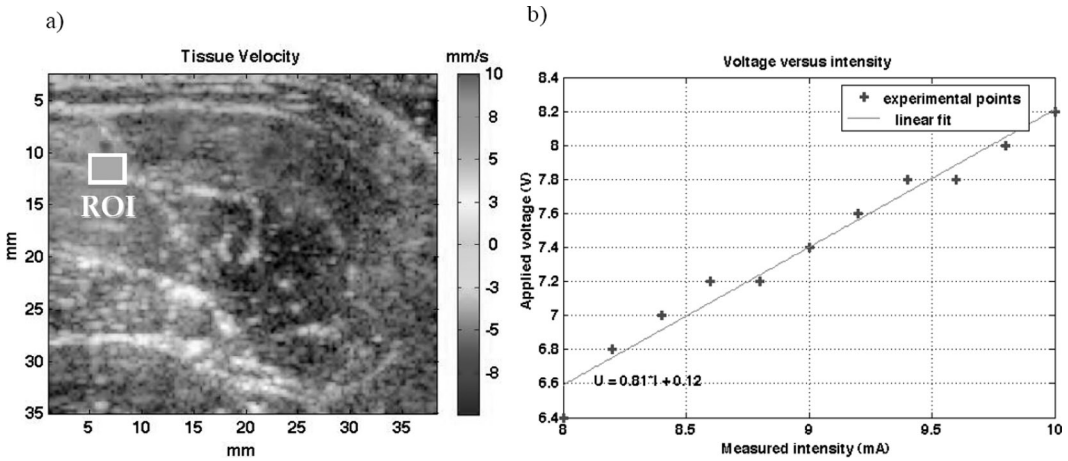

Fig. 5. (a) Tissue velocity field in a transverse image of the biceps brachii 14 ms after an 9 V (11 mA) electrostimulation. An approximately 3×3 mm^2 region of interest (ROI) is defined around the maximum. (b) Measured intensity versus applied voltage shows a quasi-constant impedance of approximately 810 Ω.

to follow the voltage meaning that the skin impedance did not change much for a given position of the electrodes [Fig. 5(b)].

2. Repeatability of Tissue Velocity Profile: To estimate the repeatability of a single electrostimulation experiment, 30 acquisitions were done with fixed amplitude (9 V) without changing the electrodes or imaging probe positions (Fig. 6).

The maximum is found to be 2.9 mm/s ± 0.2 mm/s (relative error of 6%) and the minimum at −0.9 mm/s ± 0.1 mm/s (relative error of 11%). This standard deviation is relatively low considering the *in vivo* nature of the measurements, amplified by the highly nonlinear behavior of the muscle as well as the electrostimulation strength variation. It is also not clear if the subject's ability to contract its own muscle can interfere, consciously or not. Although repeatability seems rather good, we expect reproducibility to be much lower particularly due to the position of the arm and the placement of the electrodes.

3. Influence of Stimulation Amplitude: Slowly incrementing the voltage of the electrostimulation device, the velocity field induced by the contraction was recorded. Results show that the velocity, as expected, gradually increases with the voltage, thus showing that more and more motor units are recruited [26] (Fig. 7). The *in situ* tissue velocity curves also illustrate the threshold effect of the excitation found to be around 10 mA for each volunteer.

Interestingly, maximum tissue velocity seems to depend on the square of the stimulation amplitude (Fig. 8); however, more data are needed to confirm this hypothesis. The stimulus threshold appears at 7.7 V corresponding here to 10 mA. The extracted tissue velocity profiles are very close to those obtained for typical surface mechanomyograms [12].

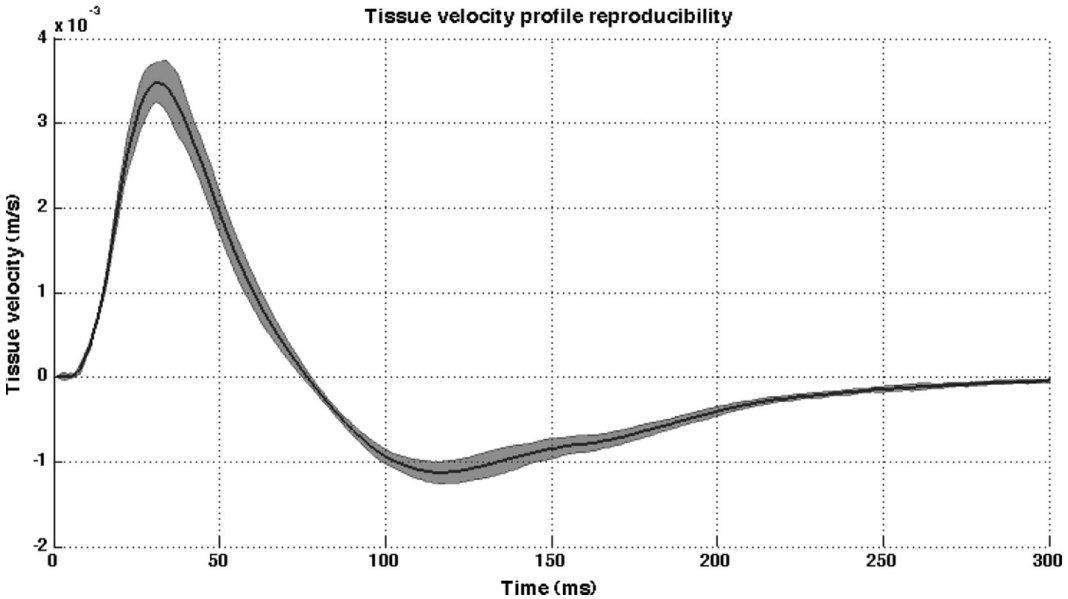

Fig. 6. Tissue velocity profile: mean of the 30 acquisitions with its standard deviation envelope. The relative error is approximately 10% at peak velocities. Total duration of these 30 acquisitions was approximately 5 min (Volunteer #2).

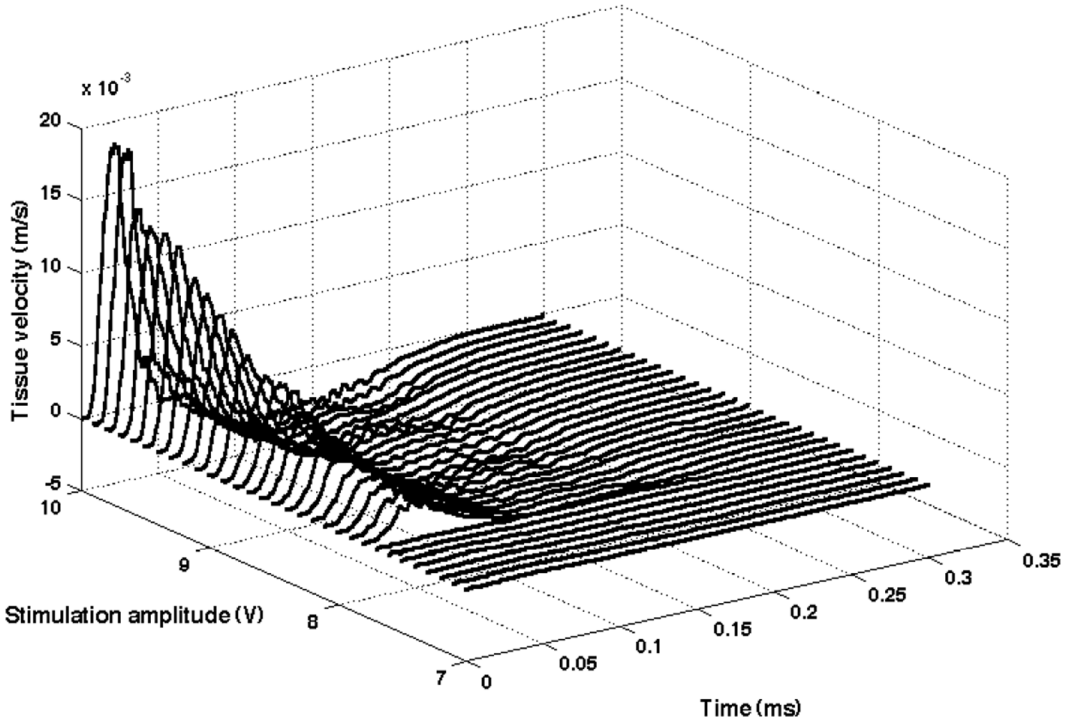

Fig. 7. Tissue velocity field versus time and stimulation amplitude. Amplitude is progressively increased from 7 to 10 V by a 0.1 V step (corresponding roughly to 8.5 mA to 12.5 mA with a 0.1 mA step). The threshold of contraction is visible for a 8 V stimulation (approximately 10 mA).

4. Inter-Subject Comparison: Measurements on 3 healthy volunteers show that the behavior is similar among all subjects, and tissue velocity field is roughly in the same range (Fig. 9). However, there seem to be differences in maximum tissue velocity field as well as on the threshold value. We speculate that these differences have, again, more to do with electrostimulation parameters [23] (mainly position) than physiological differences of the muscles.

B. Contraction and Relaxation Times

1. Definition of Characteristic Times: By extracting the velocity field in a region of interest (ROI) corresponding to the tracked fiber bundle, it is possible to display the temporal profile of the velocity field along the muscle fiber bundle (Fig. 10). This representation illustrates the contraction and its amplitude. Temporal features can also easily be extracted, such as the contraction time (when velocity is positive) and relaxation time (when velocity is negative). To do that we define characteristic points on the velocity profile.

Extraction of these characteristic points has been done through a simple procedure: first maximum and minimum of the velocity profile is computed. The start point is found thanks to a threshold on the curve and the last point is defined as half relaxation time.

2. Repeatability of Characteristic Times Measurement: Repeatability is first investigated on 30 successive acquisitions with the same stimulation amplitude; characteristic times are extracted and their standard deviations computed (Table I).

Using ultrafast imaging allows an increase in the time resolution and an improvement in the overall quality of these measurements. One can also define the contraction and half relaxation times as the part when the tissue velocity is positive and negative, respectively ($T_{contraction} = T_{zero\ crossing} - T_{start}$, $T_{relaxation} = T_{half\ min} - T_{zero\ crossing}$). The contraction and half relaxation times found in the current study match results from the literature [10] for

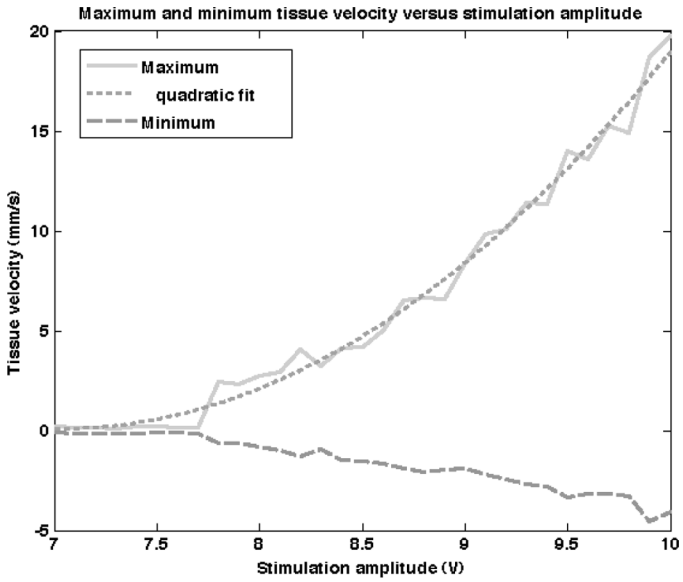

Fig. 8. Maximum and minimum of the tissue velocity field versus stimulation amplitude. A quadratic fit has been added (Volunteer #2).

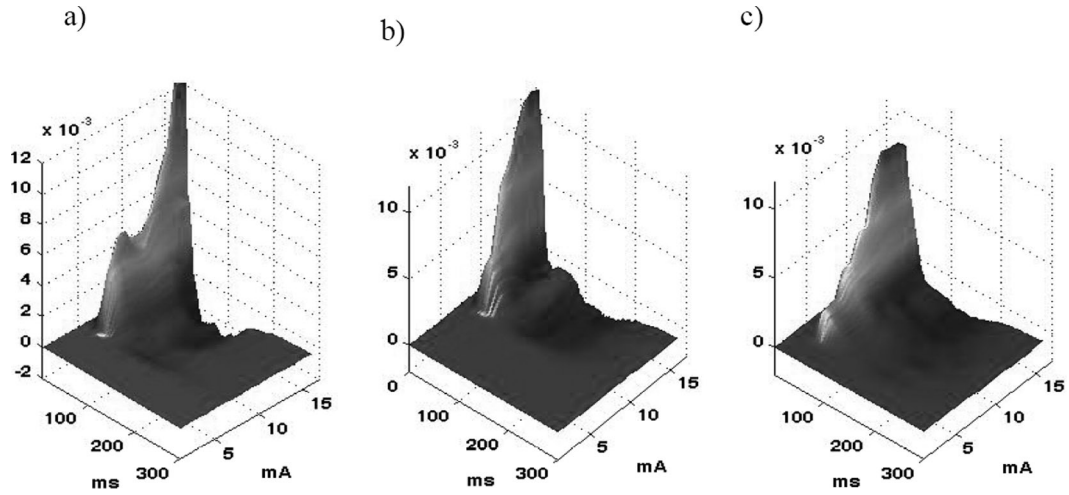

Fig. 9. Inter-subject comparison (3 volunteers) of the tissue velocity field versus time and electrostimulation intensity.

in vitro surface mechanomyograms [12] or results from *in vivo* surface mechanomyograms [19].

3. Influence of Stimulation Amplitude on Characteristic Times: The influence of the stimulation amplitude on the characteristic times was investigated (Fig. 11).

The characteristic times do not depend much on the stimulation amplitude, which should thus make their measurements more robust to the electrodes positions. On the measurable part of the graph (where tissue velocity is high enough), their values are respectively 6.2 ± 1.3 ms, 27.2 ± 4.1 ms, 69.1 ± 8.8 ms, 110.7 ± 4.7 ms and 292.5 ± 12.6 ms.

4. Inter-Subject Comparison: Ten acquisitions were done on the biceps brachii of 3 healthy volunteers using the same setup. Contraction and half relaxation times were then extracted as well as their standard deviation (Table II).

No significant differences can be noted among the 3 healthy volunteers' contraction and half relaxation times (differences are within the standard deviation range). However, comparing results of the 2 different sets of measurements on volunteer #2 (Tables I and II) together with the independence of electrostimulation amplitude and characteristic times suggest that reproducibility should be reasonable. Those measurements demonstrate *in vivo* and *in situ* measurements of the mechanical contraction and half relaxation times in a human biceps brachii. Contraction and half relaxation times correlate well with surface mechanomyography. Contraction and half relaxation times are important to measure since they are specific to the contracting fiber types, e.g., slow or fast fibers [19].

C. Tetany

These velocity profiles can also be used concurrently with a periodical electrical stimulation leading to a periodical mechanical response or a tetany of the muscle

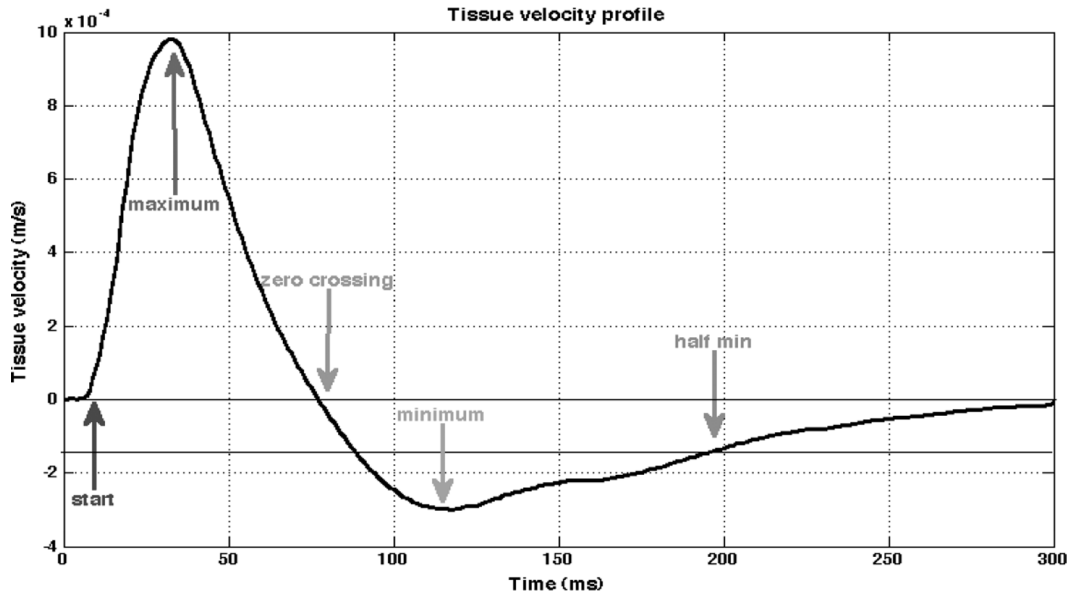

Fig. 10. Example of tissue velocity profile and definition of the extracted points (Volunteer #2).

TABLE I. REPEATABILITY OF MEASUREMENTS OF CHARACTERISTIC TIMES AND STANDARD DEVIATION (VOLUNTEER #2).

	start	maximum	zero crossing	minimum	Half min	contraction	Half relaxation
mean (ms)	7.1	30.4	77.2	115.4	182.3	**70.1**	**105.2**
standard deviation (ms)	1.2	3.2	1.6	7.8	11.3	**2**	**11**

TABLE II. MEASUREMENTS OF CONTRACTION AND HALF RELAXATION TIMES AND STANDARD DEVIATION ON THREE HEALTHY VOLUNTEERS.

	Volunteer #1	Volunteer #2	Volunteer #3
Contraction (ms)	66.3 ± 5.7	70 ± 2.3	73.4 ± 8.6
Half Relaxation (ms)	102.9 ± 11	104 ± 12.5	114.5 ± 24

depending on the frequency used for the stimulation (Fig. 12). These profiles show the tetany threshold in the stationary state of the muscle when tetany occurs.

The 1 ms electrostimulation pulse was repeated with different pulse repetition rates (from 1 to 20 Hz with a 0.5 Hz step). The velocity profiles in a 3 × 3 mm^2 ROI were acquired at 500 Hz during one l second. The data are represented as a pulse repetition rate versus time matrix [Fig. 12(a)]. Maximum amplitude of the velocity profiles have been extracted from **[AU3: AuQ: Incomplete sentence]**

Below the tetany threshold, the tissue velocity follows the excitation; above it, a summation of the response takes place and the contraction increases. In the stationary case, the muscle is fully contracted and incoherently vibrates around this position: the velocity profiles show lower amplitudes and a rich spectral content.

D. Spatial Measurements

Until now all measurements were focused on the time profile of the contraction by looking at the velocity field inside an approximatively 3 × 3 mm^2 ROI . We will now demonstrate how using a true imaging technique such as eMMG enables visualization of the spatial extension of the contracting fiber bundle and its behavior. It has an advantage over surface mechanomyography, which has to deal with the summation of responses from large areas. With eMMG, it is possible to measure the tissue velocity field inside the contracting sources.

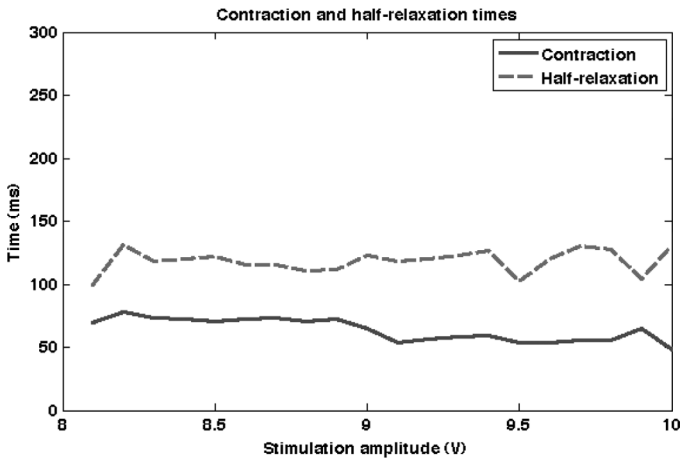

Fig. 11. Influence of the stimulation amplitude on the characteristic times (Volunteer #2).

1. Spatial Extension and Maps: Using a threshold on the tissue velocity field enables the drawing of curves that illustrate the spatial extension of the contracting area (Fig. 13). This moving area consists of the true contracting bundle and the passive surrounding elastic tissue.

2. Twist of the Tissue: Many acquisitions clearly show a twist of the contracting fiber bundle (Fig. 14); the measured component of the tissue velocity is positive and negative side by side in the image, following the contraction dynamics, and the phenomenon is then reversed during the relaxation. Whether the twist is due to the contractile tissue itself or to hard boundary conditions at the end of the fiber bundles is unknown.

Geometrical features that cannot be visualized by surface mechanomyograms are available.

E. 3-D Fiber Bundle Tracking and Visualization

By performing a 3-D stroboscopic scan along the biceps, a whole volume of the tissue velocity field can be acquired. We chose to scan 22 positions with a 2-mm step for a total scanned volume of 44 × 38 × 50 mm^3 (Fig. 15); a 1500 Hz frame rate was used. Results show that the tissue velocity distribution mainly follows a curve that matches visible echogeneic structures and is thought to be a fiber bundle. The coordinates of this curve are automatically extracted and the equation of encompassing planes computed. These coordinates are useful for 3-D visualization of the data as well as for the reconstruction of the tissue velocity profile along the fiber bundle [Fig. 15(b)]. We can reconstruct then contracting fiber bundle using an isosurface.

These results show the feasibility of the *in vivo* tracking of a contracting fiber bundle with a low electrically

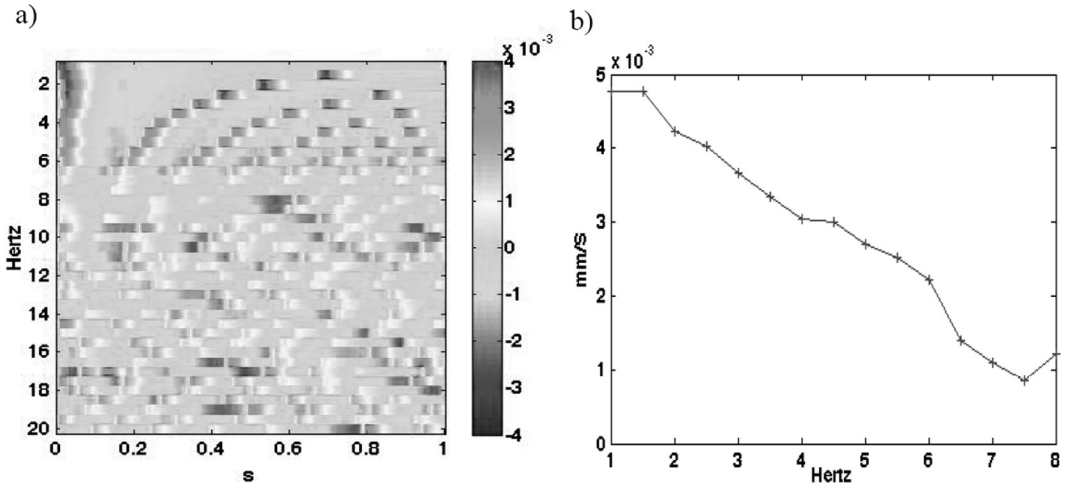

Fig. 12. (a) Response of the muscle to different excitation frequencies. Its behavior becomes erratic at greater than 7.5 Hz. (b) Tissue velocity maximum amplitude versus excitation frequency.

induced stimulation. The localization of the contracting fiber bundle is retrieved in a 3-D volume and matches echogeneic structures of the muscle (Fig. 16). This represents the first attempt of tracking contracting muscle fibers *in vivo*. Diffusion tensor imaging, an MR imaging-based technique has been applied to the anatomical tracking of skeletal muscle fibers [27], but can give only anatomical information and no functional information on the mechanical response of a muscle to a given stimulation.

However, this experiment is difficult in practice. Choosing the right position for the arm, the probe, and the electrodes and good electrostimulation parameters inside the water tank is tricky and uncomfortable, whereas moving the probe directly on the skin leads to changes in the electrostimulation strength and a drop in repeatability, thus preventing a stroboscopic acquisition.

IV. Discussion

From a similar experiment acquired every millimeter with a 2000 Hz frame rate, we have been able to extract characteristic times inside the contracting area, such as the maximum, the zero crossing, and the minimum times, every millimeter along 2 cm of the biceps brachii (Fig. 17).

These velocity profile maxima, zeros, and minima can be fitted to straight lines (Fig. 17, right); the slope of each series of points gives respectively propagation velocities of 4.2, 3.3 and 3.8 m/s. The accuracy of this measurement is highly limited by the width of the signal, and the range of velocity requires a high frame rate.

It is striking to compare such measured velocities to other characteristic propagation velocities of the biceps brachii muscle, muscle fiber conduction velocity, and shear wave velocity.

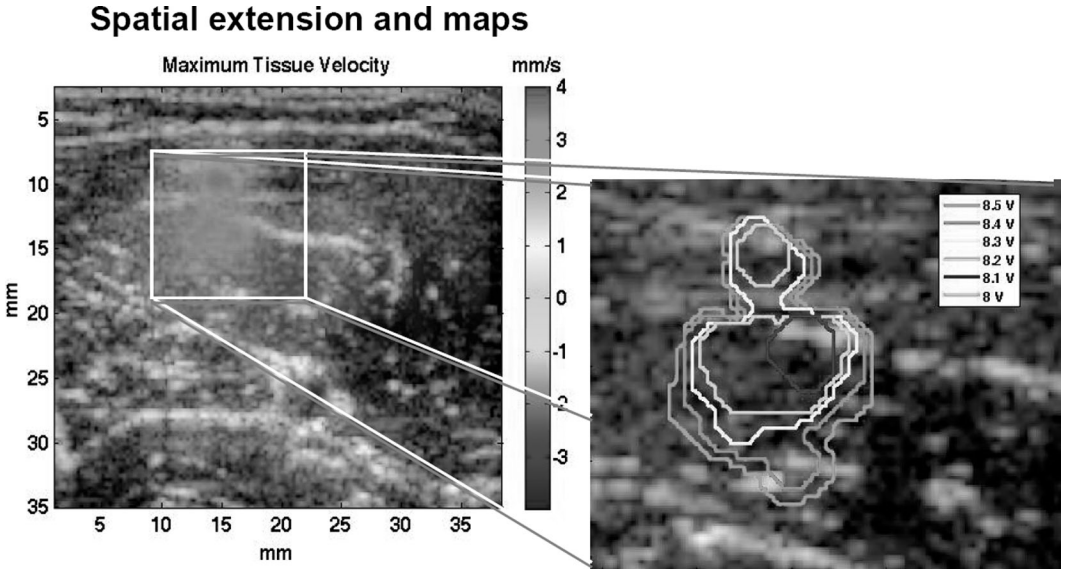

Fig. 13. Map (left) of the maximum of the tissue velocity field (8.3 V stimulation) and spatial extension (right) of the contraction as visualized by an isocontour on the velocity tissue field. A threshold of 2 mm/s was used.

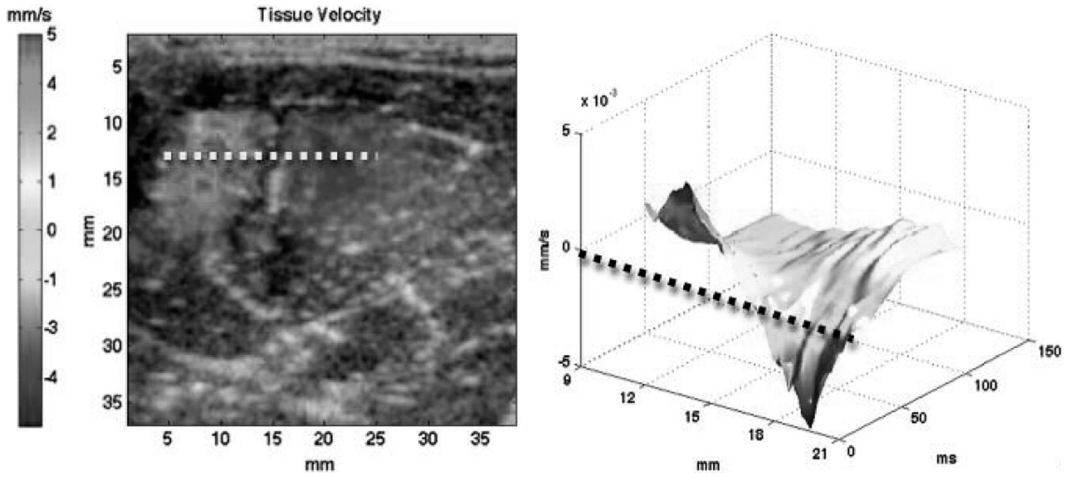

Fig. 14. Illustration (left) of the twist of a contracting fiber bundle. Red means going up whereas blue means going down. The projected components (right) of a clockwise rotation are visible, and the associated time profiles along a sample line (dashed line) illustrate the anticlockwise rotation during relaxation.

An application of electromyography well known by muscle physiologists and named muscle fiber conduction velocity (MFCV) enables the measurement of the velocity of action potentials traveling along the muscle fibers. The electromyography signals recorded by an array of electrodes on the muscle surface are correlated; from the time shift between 2 positions, a velocity of the underlying electrical wave can be computed. This "wave" called M-wave is found to have a velocity ranging from 3.5 to 5.5 m/s [11] in the biceps brachii. The striking similitude between the electric and mechanic propagation is not that surprising since the mechanical response is thought to be triggered by the M-wave.

Another characteristic velocity can play a role in the observed phenomenon, mechanical shear waves. Shear waves or transversal waves propagate in soft tissues between 1 and 10 m/s a thousand times slower than longitudinal waves (1500 m/s); moreover, their velocities are directly linked to the stiffness of the material. To measure the shear velocity of an *in vivo* biceps brachii (Volunteer #3) along the fibers, the same echograph was simply put in the supersonic shear imaging mode [20] and all electrostimulation devices were shut down. For illustrative purposes, the subject was asked either to stay relaxed or to carry a 4 kg load. Details measurements on the biceps brachii are beyond the scope of this paper and will be provided in a following paper. A quick analysis of the shear wave profiles show a propagation velocity of 2 m/s with no load and 4 m/s with the 4 kg load, illustrating that the muscle is getting stiffer with the contraction strength (Fig. 18). These velocities, especially when the muscle is contracting, are very close to the velocity measured and to the much more known M-wave velocity.

By combining the measurements of electrostimulated muscle contraction with local elasticity estimation of passive muscular tissue [20] on the same probe, it should be possible to understand if the mechanical pattern recorded during this electrostimulation experiment is due either to the single propagation of the action potential, to the propagation of mechanical shear waves due to the contraction, or, more interestingly, to a natural and clever coupling of both waves. In particular, this resulting mechanical wave could be an elegant way to increase excitability along the skeletal muscle fiber by mechanically triggering stretch-ac-

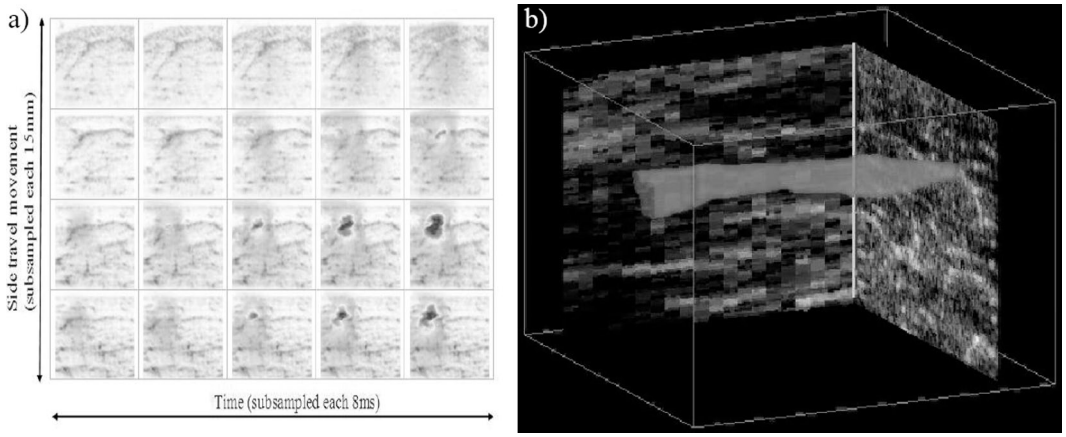

Fig. 15. (a) Raw data acquired in the transverse plane (38 × 50 mm). (b) Fiber bundle's envelope extraction after thresholding at 80% of the maximum of each renormalized transverse acquisition.

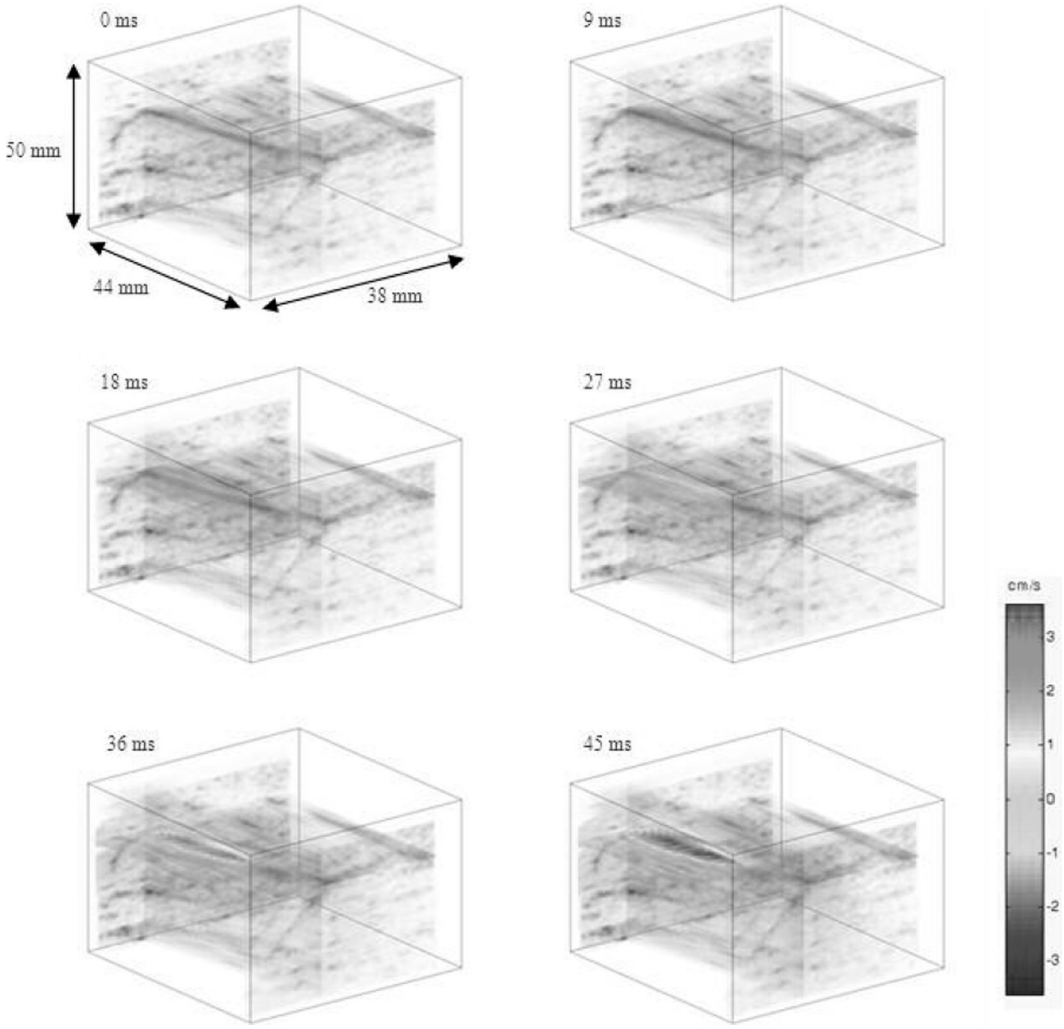

Fig. 16. A 3-D visualization of the tissue velocity field at various times after electrostimulation. The contraction of a fiber bundle is clearly visible and matches echogeneic structures.

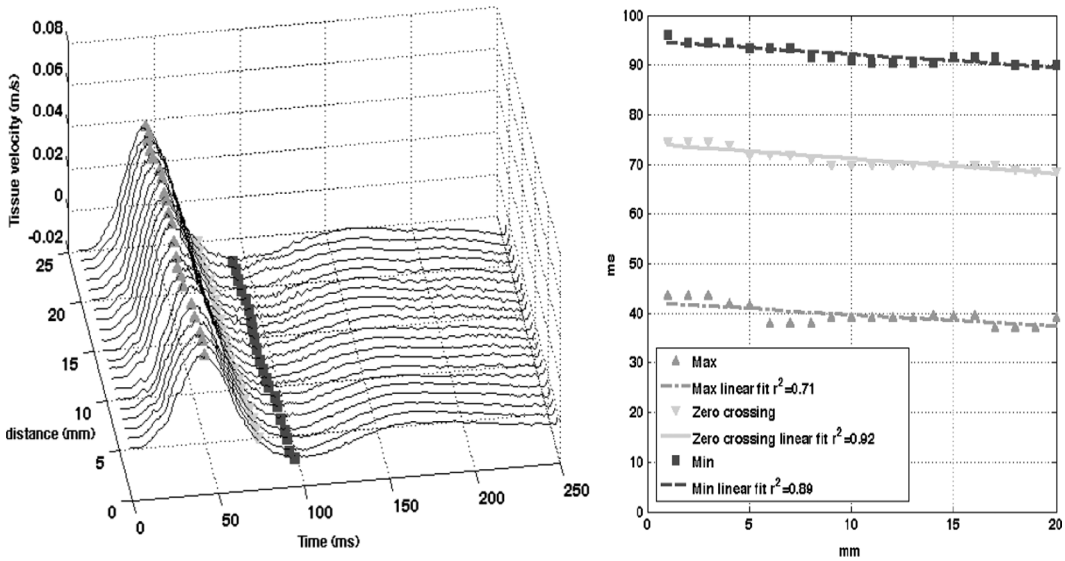

Fig. 17. Electrostimulation. Left: visualization of the velocity profile for different positions along the biceps brachii (Volunteer #3). Right: a linear fit of the characteristic points of the curve at a propagation velocity of approximately 4 m/s.

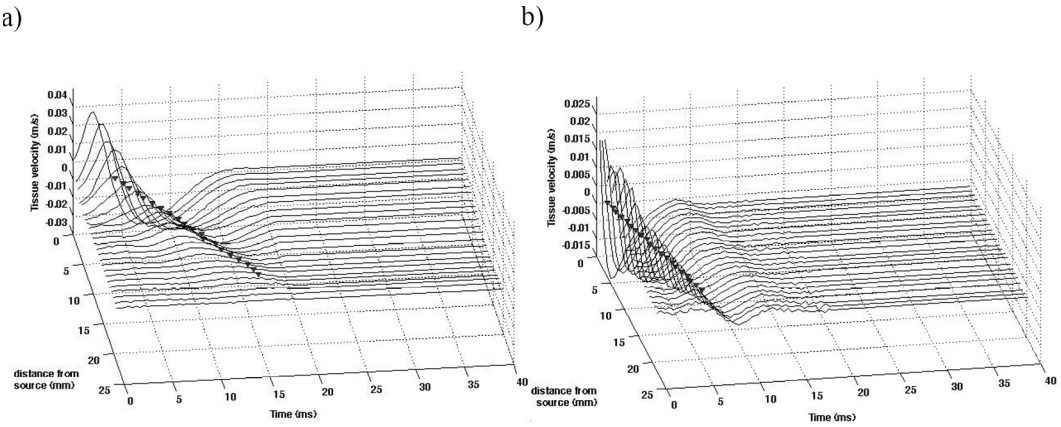

Fig. 18. No electrostimulation. The supersonic shear imaging technique is applied on an *in vivo* biceps brachii parallel to the fibers (Volunteer #3) to initiate and follow a shear wave. (a) Velocity profile when muscle is in rest state; shear velocity is 2 m/s. (b) A 4 kg load is applied; shear velocity increases to 4 m/s.

tivated ion channels [28], a mechanism known as the myogenic response for cardiac [29] and smooth [30] muscles.

V. Conclusion

The clinical emergence of ultrafast scanners could soon propose echo mechanomyography as a unique and original way of imaging the transient mechanical response of a muscle to an electrical stimulation. Using very high frame rate ultrasound, the contractile properties of a fiber bundle can be fully measured *in situ*, imaged, and tracked in 2D or 3-D, upgrading surface mechanomyography to *in depth* imaging with optimal time and spatial resolutions for *in vivo* applications. It permits both the *in situ* estimation of muscle fiber conduction speed and the localization of muscle fibers recruitment. The technique now needs to be tested with standard electrostimulation procedures used by surface mechanomyography studies to compare and improve results. It could then lead to a new *in situ* tool for muscle physiologists. Coupled with electromyography, clinicians would have both the electrical command and the *in situ* mechanical response of a muscle, information that could improve diagnosis and monitoring of neuromuscular diseases.

References

[1] R. L. Segal, "Use of imaging to assess normal and adaptive muscle function," in *Phys. Ther.*, vol. 87, no. 6, pp. 704–718, June. 2007.

[2] M. J. Aminoff, *Electromyography in Clinical Practice*, 3rd ed. New York: Churchill Livingstone, 1987**[AU4: Aminoff's 2nd ed. was in 1987; his 3rd ed. was in 1998; which is correct here?]**.

[3] C. Orizio, "Muscle sound: Bases for the introduction of a mechanomyographic signal in muscle studies," in *Crit. Rev. Biomed. Eng.*, vol. 21, no. 3, pp. 201–243, 1993.

[4] J. Viby-Mogensen, E. Jensen, M. Werner, and H. K. Nielsen, "Measurement of acceleration: A new method of monitoring neuromuscular function," in *J. Clin. Anesth.*, vol. 15, no. 2, pp. 145–148, Mar. 2003.**[AU5: There is a problem with this ref.; either these authors and title go with Acta Anesthesiol. Scand., vol. 32, no. 1, pp. 45–48, Jan. 1988 - or -]**

[5] C. Patten, R. A. Meyer, and J. L. Fleckenstein, "T2 mapping of muscle," in *Semin. Musculoskelet. Radiol.*, vol. 7, no. 4, pp. 297–305, Dec. 2003.

[6] R. Taylor, T. B. Price, D. L. Rothman, R. G. Shulman, and G. I. Shulman, "Validation of 13C NMR measurement of human skeletal muscle glycogen by direct biochemical assay of needle biopsy samples," in *Magn. Reson. Med.*, vol. 27, no. 1, pp. 13–20, Sep. 1992.

[7] G. P. Pappas, D. S. Asakawa, S. L. Delp, F. E. Zajac, and J. E. Drace, "Nonuniform shortening in the biceps brachii during elbow flexion," in *J. Appl. Physiol.*, vol. 92, no. 6, pp. 2381–2386, June. 2002.

[8] M. A. Dresner, G. H. Rose, P. J. Rossman, R. Muthupillai, A. Manduca, and R. L. Ehman, "Magnetic resonance elastography of skeletal muscle," in *J. Magn. Reson. Imaging*, vol. 13, no. 2, pp. 269–276, Feb. 2001.**[AU6: This ref. has been changed; is it correct now?]**

[9] N. R. Grubb, A. Fleming, G. R. Sutherland, and K. A. Fox, "Skeletal muscle contraction in healthy volunteers: Assessment with Doppler tissue imaging," in *Radiology*, vol. 194, no. 3, pp. 837–842, Mar. 1995.

[10] S. Pillen, M. van Keimpema, R. A. J. Nievelstein, A. Verrips, W. van Kruijsbergen-Raijmann, and M. J. Zwarts, "Skeletal muscle ultrasonography: Visual versus quantitative evaluation," in *Ultrasound Med. Biol.*, vol. 32, no. 9, pp. 1315–1321, Sep. 2006.

[11] D. Farina, W. Muhammad, E. Fortunato, O. Meste, R. Merletti, and H. Rix, "Estimation of single motor unit conduction velocity from surface electromyogram signals detected with linear electrode arrays," in *Med. Biol. Eng. Comput.*, vol. 39, no. 2, pp. 225–236, Mar. 2001.**[AU7: No Ref. [11] in original manuscript. Refs. have been renumbered to include [11]. Please proof carefully.]**

[12] Y. Yoshitake, M. Shinohara, H. Ue, and T. Moritani, "Characteristics of surface mechanomyogram are dependent on development of fusion of motor units in humans," in *J. Appl. Physiol.*, vol. 93, no. 5, pp. 1744–1752, Nov. 2002.

[13] R. S. Witte, D. E. Dow, R. Olafsson, Y. Shi, and M. O'Donnell, "High resolution ultrasound imaging of skeletal muscle dynamics and effects of fatigue," in *Proc. IEEE Ultrason. Symp.,* vol. 1, Aug. 2004, pp. 764–767.

[14] R. S. Witte, K. Kim, B. J. Martin, and M. O'Donnell, "Effect of fatigue on muscle elasticity in the human forearm using ultrasound strain imaging," in *Proc. IEEE Int. Conf. Eng. Med. Biol. Soc.*, vol. 1, Aug. 2006, pp. 4490–4493.

[15] T. Deffieux, J.-L. Gennisson, M. Tanter, and M. Fink, "Ultrafast imaging of *in vivo* muscle contraction using ultrasound," in *Appl. Phys. Lett.*, vol. 89, no. 18, art. no. 184107, Nov. 2006.

[16] L. Sandrin, M. Tanter, S. Catheline, and M. Fink, "Shear modulus imaging with 2-D transient elastography," in *IEEE Trans. Ultrason., Ferroelect., Freq. Contr.*, vol. 49, no. 4, pp. 426–435, Apr. 2002.

[17] A. Sandow, "Electromechanical transforms and the mechanism of excitation-contraction coupling," in *J. Mechanochem. Cell Motil.*, vol. 2, no. 3, pp. 193–207, Nov. 1973.

[18] J. V. Basmajian and C. J. De Luca, *Muscles Alive: Their Functions Revealed by Electromyography*, 2nd ed. Baltimore: *Williams &Wilkins,* 1985.
[19] A. Eberstein and J. Goodgold, "Slow and fast twitch fibers in human skeletal muscle," in *Am. J. Physiol.*, vol. 215, no. 3, pp. 535–541, Sep. 1968.
[20] J. Bercoff, M. Tanter, and M. Fink, "Supersonic shear imaging: A new technique for soft tissue elasticity mapping," in *IEEE Trans. Ultrason., Ferroelect., Freq. Contr.*, vol. 51, no. 4, pp. 396–409, Apr. 2004.
[21] M. Tanter, J. Bercoff, L. Sandrin, and M. Fink, "Ultrafast compound imaging for 2D motion vector estimation: Application to transient elastography," in *IEEE Trans. Ultrason., Ferroelect., Freq. Contr.*, vol. 49, no. 10, pp. 1363–1374, 2002.
[22] J. Ophir, I. Cespedes, H. Ponnekanti, Y. Yazdi, and X. Li, "Elastography: A quantitative method for imaging the elasticity of biological tissues," in *Ultrason. Imag.*, vol. 13, pp. 111–134, Apr. 1991.
[23] B. J. Forrester and J. S. Petrofsky, "Effect of electrode size, shape, and placement during electrical stimulation," in *J. Appl. Res.*, vol. 4, no. 2, pp. 346–354, 2004.
[24] J. L. Gennisson, C. Cornu, S. Catheline, and M. Fink, "Human muscle hardness assessment during incremental isometric contraction using transient elastography," in *J. Biomech.*, vol. 38, no. 7, pp. 1543–1550, July. 2005.
[25] Y. C. Fung, *Biomechanics: Mechanical Properties of Living Tissues*, 2nd ed. New York: Springer, 1993.
[26] S. J. Dorgan and M. J. O'Malley, "A mathematical model for skeletal muscle activated by N-let pulse trains," in *IEEE Trans. Rehabil. Eng.*, vol. 6, no. 3, pp. 286–299, Sep. 1998.
[27] C. C. Van Donkelaar, L. J. G. Kretzers, and P. H. M. Bovendeerd, "Diffusion tensor imaging in biomechanical studies of skeletal muscle function," in *J. Anat.*, vol. 194, no. 1, pp. 79–88, Jan. 1999.
[28] N. Mallouk and B. Allard, "Stretch-induced activation of Ca^{2+}-activated K^+ channels in mouse skeletal muscle fibers," in *Am. J. Physiol. Cell Physiol.*, vol. 278, no. 3, pp. C473–C479, Mar. 2000.
[29] H. Hu and F. Sachs, "Stretch-activated ion channels in the heart," in *J. Mol. Cell. Cardiol.*, vol. 29, no. 6, pp. 1511–1523, June. 1997.
[30] M. J. Davis, J. A. Donovitz, and J. D. Hood, "Stretch-activated single-channel and whole cell currents in vascular smooth muscle cells," in *Am. J. Physiol. Cell Physiol.*, vol. 262, no. 4, pp. C1083–C1088, Mar. 1992.

Thomas Deffieux was born in 1982 in Paris, France. He received his MsC. degree in physics and image processing in 2005 from the University Louis Pasteur of Strasbourg. Since 2005, he is a Ph.D. student, directed by Mathias Fink, at the Laboratoire Ondes et Acoustique (ESPCI) in Paris, France. His current research fields include ultrafast ultrasonic imaging and quantitative elastography of soft tissues by shear wave propagation (supersonic shear imaging) applied to *in vivo* breast, liver, and muscle tissues.

Jean-Luc Gennisson was born in 1974 in France. He received the DEA degree in electronics in 2000 from the University of Paris VI. In 2003, he received the Ph.D. degree in physics (acoustics) from the University of Paris VI for his work on elastography. From 2003 to 2005, he worked at the laboratory of biorheology and medical ultrasound in Montreal carrying out postdoctoral research with Pr. Guy Cloutier. In 2005, he became a research scientist of the French National Research Center (CNRS). His current research interests include medical ultrasonic imaging, shear wave propagation in soft tissues for cancer detection, and nonlinear shear waves.

Mickaël Tanter was born in December 1970 in Paimpol, France. He received the engineering degree in electronics from Ecole Supérieur d'Electricité (SUPELEC) in 1994. In 1999, he received the Ph.D. degree in physics (acoustics) from the University of Paris VII for his work on the application of time reversal to ultrasonic brain therapy and the "Habilitation de Recherche" in 2004. From 2000 to 2005, he was an associate research professor at the French Center for Scientific Research (CNRS) at ESPCI (Ecole Supérieure de Physique et de Chilie Industrielle), Paris, France. In 2005, he became a research professor at the French Institute for Medical Research (INSERM). He is currently the head of the research team "Wave Physics for Medicine" at the Laboratoire Ondes et Acoustique (ESPCI) laboratory, directed by Mathias Fink. His current research interests include ultrasonic imaging and therapy (adaptive focusing techniques in heterogeneous media, medical ultrasonic imaging, ultrasonic brain imaging, shear wave propagation in soft tissues for cancer detection, ultrasonic therapy, nonlinear acoustics, and active noise control). He holds 7 patents in the field of ultrasound and he has published more than 50 articles. He is a co-founder of the start-up company SuperSonic Imagine in the field of medical ultrasound.

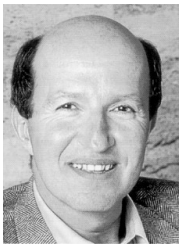

Mathias A. Fink received the diplome de Doctorat de $3^{\text{ème}}$ cycle in solid state physics in 1970 and the Doctorat ès-Sciences degree in acoustics in 1978 from Paris University, France. From 1981 to 1984, he was a professor of acoustics at Strasbourg University, France. Since 1984, he has been a professor of physics at Paris University (Denis Diderot), France. In 1990 he founded the Laboratoire Ondes et Acoustique at the Ecole Supérieure de Physique et de Chimie Industrielles de la Ville de Paris (ESPCI). In 1994, he was elected to the Institut Universitaire de France. His current research interests include medical ultrasonic imaging, ultrasonic therapy, nondestructive testing, underwater acoustics, active control of sound and vibration, analogies between optics and acoustics, wave coherence in multiple scattering media, and time reversal in physics. He has developed different techniques in speckle reduction, in wave focusing in inhomogeneous media, and in ultrasonic laser generation. He holds 20 patents, and he has published more than 220 articles. In 2003, he was elected to the French Academy of Science.